Synthesis and Evaluation of New Iodine-125 Radiopharmaceuticals as Potential Tracers for Malignant Melanoma

Josette M. Michelot, Marie-France C. Moreau, Pierre G. Labarre, Jean-Claude Madelmont, Annie J. Veyre, Janine M. Papon, Daniel F. Parry, Jacques F. Bonafous, Jean-Yves P. Boire, Gérard G. Desplanches, Suzanne J. Bertrand, and Gaston Meyniel

INSERM U 71, B.P. 184, Clermont-Ferrand, France; Centre Jean Perrin, B.P. 392, Clermont-Ferrand, France; Département de Biomathématiques, Faculté de Médecine, B.P. 38, Clermont-Ferrand, France; CIS bioindustries, B.P. 6, Gif-sur-Yvette Cedex, France; and INSERM U 218, Centre Léon Bérard, Lyon, France.

The synthesis, labeling, and biodistribution of four ^{125}I radiopharmaceuticals designed to localize in melanoma were tested. Uptake in tumors was demonstrated by autoradiography of whole-body sections and quantitated by measurement of radioactivity of selected tissues and tumors using melanoma-bearing mice. *N*-(2-diethylaminoethyl)-4-iodobenzamide was selected for its highest melanoma uptake: 60 min after IV injection of 6.5% and 4% ID/g, respectively for murine B16 and human melanotic melanoma. Tumor uptake showed the highest values of all analyzed tissues from 6 to 24 hr after injection. High uptake in melanotic tumor tissue with relatively low uptake in blood, muscle, brain, lung, and liver tissue resulted in high tumor/nontumor ratios (at 24 hr for B16, tumor/blood = 37, tumor/brain = 147, tumor/muscle = 95). This agent was compared with iodoamphetamine. Scintigraphic images of the tumor confirmed that external detection of melanoma is possible with this new radiopharmaceutical.

J Nucl Med 1991; 32:1573–1580.

Owing to the aggressive nature of malignant melanoma, early detection of invasion and metastatic process is of paramount importance (*1,2*). In an effort to meet the objective of early detection, researchers and clinicians have used radiolabeled monoclonal antibodies (MAb) that bind to specific melanoma associated antigens. This process of radioimmunoimaging has been reported extensively in the literature (*3–9*). However, a basic understanding of the kinetics and tumor localizing properties of MAb and associated fragments has yet to be clearly articulated.

The radiopharmaceutical most widely used for tumor detection has been [^{67}Ga] citrate, a nonspecific tumor imaging agent (*10,11*). In experimental tumors, imaging with [^{67}Ga] citrate has been performed with both melanotic and amelanotic melanoma, but results in patients have been modest.

Radiopharmaceuticals with affinity for melanin have been developed but to date none has achieved clinical application for the early detection of metastases (*12–14*). Because of a known melanotropic affinity and selective localization in the pigmented structures of the eyes, iodoquinoline derivatives labeled with ^{125}I or ^{123}I have been tested in animal models, but, again, the detection of skin and ocular melanoma has had limited success (*15,16*). Thiouracil has been shown to be selectively incorporated into the melanin pigment of melanoma by serving as a false melanin precursor. Coderre et al. (*17*) observed iodothiouracil incorporation into remote secondary metastases using a metastatic melanoma cell line. A recent patient study testing the efficiency of radioiodine labeled 5-iodo-2-thiouracil as a diagnostic agent was carried out by van Langevelde (*18*). However, preliminary results did not warrant continued use of this radiopharmaceutical. *N*-isopropyl-p-iodoamphetamine (IMP) used primarily for brain imaging, is found to be associated with eye uptake in animals. Recent works by Wada et al. (*19*) and Cohen et al. (*20*) reported detection of both primary and metastatic malignant melanoma with [^{123}I]IMP.

In a previous work (*21*) concerning new brain-seeking radiopharmaceuticals, we developed a series of aromatic iodinated amino compounds labeled with [^{125}I] (Fig. 1). Autoradiographic study performed after intravenous injection of the molecules in pigmented C57BL6 mice showed selective localization, for four derivatives (Fig. 2): *1*(c)–*4*(c), of the radioactivity not only in the brain, but also in the melanoid structures of the uveal tract. This phenomenon, which is not observed in Wistar albino rats, prompted us to focus our attention upon their possible uptake in melanoma. We have investigated the in vivo distribution of murine melanoma and human malignant melanoma heterotransplants after the intravenous administration of the four iodinated compounds and established a comparison between one of them and IMP. Athymic

Received July 20, 1990; revision accepted February 11, 1991.
For reprints contact: J. Michelot, INSERM U 71, Rue Montalembert, B.P.184, 63005 Clermont-Ferrand Cedex.

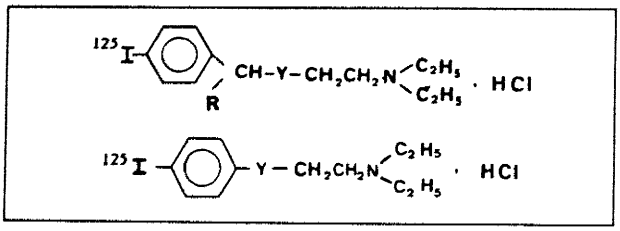

FIGURE 1. Structure of iodinated compounds: R = C_6H_5; H
Y = —COO—;—CONH—;—O—.

nude mice served as the animal model from which the study of human tumor affinity could commence. Xenografted human tumors grown in athymic nude mice maintain their karyotype, histologic appearance and most biochemical characteristics (*22,23*).

Therefore, the general purpose of the present research is to establish the effectiveness of new radiopharmaceuticals (*24*) labeled with γ-emitters as a noninvasive technique of malignant melanoma and metastasis visualization.

MATERIALS AND METHODS

Radiopharmaceuticals

The radioiodinated derivatives were prepared from the correspondent amines by the dediazoniation procedure (*25*). The Sandmeyer reaction was used for compounds *1*(c), *2*(c), *4*(c) and the Wallach triazene method for *3*(c), using the following sequence reactions.

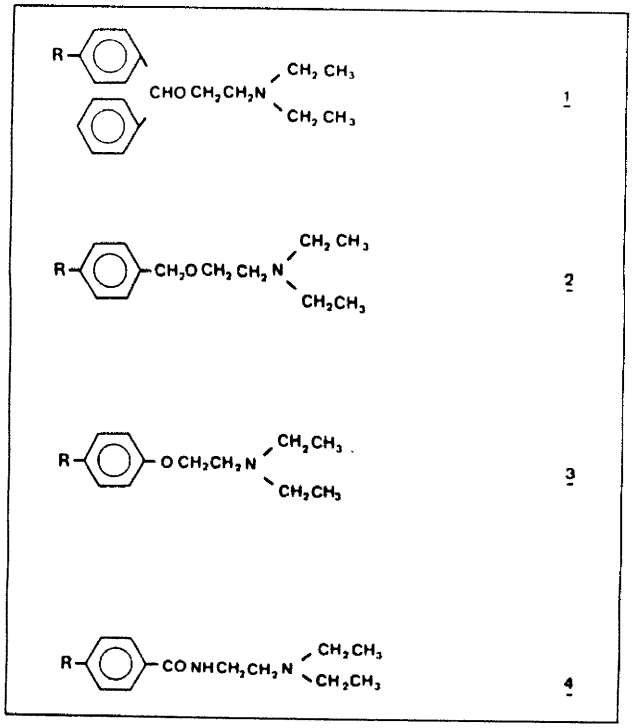

FIGURE 2. The four iodinated compounds selected for animal experimentation and their synthesis intermediates: (a) R = NO_2; (b) R = NH_2; (b′) R = N—N(C_2H_5)$_2$; and (c) R = ^{125}I.

Synthesis of Nitroderivatives ***1(a)–4(a).*** The starting nitroethers *1*(a) and *2*(a) were synthesized according to a method described by Benedict et al. (*26*) by the reaction of 2-diethylaminoethanol with respectively 4-nitrodiphenyl bromomethane and 4-nitrobenzyl bromide, in dimethyl sulfoxide, in the presence of potassium hydroxide. The nitroether *3*(a) was obtained by reacting 4-nitrophenol with 2-diethylamino ethyl chloride in acetone-water with potassium carbonate as a base. The synthesis of *4*(a) was performed by treatment of 4-nitrobenzoic acid chloride with 2-diethylaminoethyl amine in tetrahydrofuran at room temperature.

Synthesis of the Amino Intermediates ***1(b)–4(b).*** The nitro group of *1*(a) and *2*(a) was reduced with tin chloride in concentrated hydrochloric acid at 0°C. The conversion of *3*(a) and *4*(a) to the correspondent amines was accomplished by catalytic hydrogenation with 5% palladium on charcoal in absolute ethanol under normal pressure.

Synthesis of the ^{125}I*-Labeled Compounds* ***1(c)–4(c).*** The above amino agents were diazotized using sodium nitrite and concentrated hydrochloric acid at 0°C. Then the diazonium salts generated from *1*(b), *2*(b), and *4*(b) were decomposed by treatment with a solution containing potassium iodide and sodium iodide-^{125}I. The resulting radioiodinated substances were isolated with a radiochemical yield of 38% for *1*(c), 35% for *2*(c), and 45% for *4*(c) after purification by low-pressure liquid chromatography. The diazonium salt prepared from *3*(b), on coupling with a slight excess of diethylamine, gave the expected triazene *3*(b′). Treatment of *3*(b′) with trimethylsilyl iodide-^{125}I (produced in situ by the reaction of trimethylsilyl chloride with sodium iodide-^{125}I) in acetonitrile at 60°C resulted in the formation of *3*(c) in 65% radiochemical yield after column chromatography.

The four iodinated substances obtained as free amines were converted into hydrochlorides after treatment by anhydrous ethereal hydrochloric acid solution, and dissolved in physiologic saline for animal experiments.

Thin-layer chromatographic analysis (TLC) (Merck Kieselgel 60F254 plates) developed with the different solvent mixtures, chloroform–methanol (80:20 and 50:50) showed them to be identical to the authentic nonradioactive compounds and to be free of significant radiochemical impurities. Specific activity was in the range of 2.3 mCi (85 MBq)/m*M*.

Synthesis of ***4(c)*** *by Isotopic Exchange Procedure.* Nonradioactive *N*-(2-diethylaminoethyl)4-iodobenzamide was obtained by reacting 4-iodobenzoyl chloride with 2-diethylaminoethyl amine in tetrahydrofuran at room temperature (*21*).

Radiolabeling: To a solution of the above compound (10 mg) in 0.05 *M* citrate buffer at pH 4 (0.5 ml) were added 1 mCi (37 MBq) of Na^{125}I (no-carrier-added in NaOH; CIS bioindustries) and 0.5 mg of copper sulfate used as a catalyst. The reaction mixture was heated at 150°C for 35 min. Radiochemical purity was determined by silica gel over pressure TLC with the mixture chloroform–methanol–formic acid (80:20:0.5) as eluant (R_f *4*(c) = 0.45, R_f (^{125}I) = 0.1) and confirmed by high-performance liquid chromatography (HPLC) (Hewlett-Packard HP 1090) using the following system: reverse-phase column Whatman 5 OD S 3 (125 mm × 2 mm) mobile phase constituted of a gradient starting from A:B (60:40; A = 0.05 *M* sodium acetate, B = methanol) to 100% B in 8 min, followed by 100% B, at a flow rate of 1.5 ml/min (Rt *4*(c) = 11.3 min, Rt (^{125}I) = 1.8 min). Compound *4*(c) was shown to contain less than 5% of inorganic iodide and no trace of other radiochemical impurities. Thus a further purifica-

tion was not necessary and the crude mixture could be directly utilized for animal studies after dissolution in physiologic saline. Specific activity was in the range of 36 mCi (1.33 GBq)/m*M*. [^{125}I]IMP was provided by CIS bioindustries.

Animal Model and Experimental Procedure

Tumor uptake was studied in C57BL6 male mice (Iffa Credo, France) bearing the B16 melanoma and in outbred Swiss nu/nu male mice (Iffa Credo, France) bearing two human melanoma heterotransplants.

Transplantable B16 mouse melanotic melanoma was originally obtained from ICIG (Villejuif, France) and was maintained in our laboratory by serial transplantations at 3- or 4-wk intervals into 6-wk-old male C57BL6 mice. Two weeks after tumor transplantation, mice were used as donors. The tumor was first dissociated in saline solution and next filtered. Then 10^6 cells in 0.1 ml saline solution were injected subcutaneously (s.c.) on the left flank. Ten days later, the tumors became palpable, the percentage of tumor take being was 98–100%.

Six-week-old outbred Swiss *nu/nu* male mice were used for xenografts. Bedding material was sterilized before use and the cages were covered by an air filter (Isocap, Iffa Credo). The human melanoma cell lines M3Dau (amelanotic) and M4Beu (melanotic) were established in the laboratory of J.F. Doré (INSERM U 218, Centre Léon Bérard, Lyon, France) from metastatic tumors, and have been previously characterized as tumorigenic in nude mice (*27,28*). Both cell lines were maintained in vitro as monolayers in McCoy 5A and RPMI 1640 tissue culture medium, respectively, supplemented with 10% fetal calf serum, 2 m*M* glutamine, 100 I.U./ml^{-1} penicillin and 50 μg ml^{-1} streptomycin; $2 \cdot 10^6$ viable human melanoma cells in 0.1 ml PBS were inoculated s.c. in the abdomen of nude mice. Tumor growth rate was determined by weekly measuring of two perpendicular diameters of the tumor for about 4 wk. Tumor showed encapsulated growth. Local or distant metastases were never observed.

Autoradiography

At intervals, tumor-bearing C57BL6 or *nu/nu* mice injected with ^{125}I-labeled compounds were frozen at −180°C under ether anaesthesia. They were subjected to whole body sectioning according to the methodology described by Ullberg (29). The sections were exposed to X-ray film type Hyperfilm ^{3}H (RPN 535 Amersham, UK).

Biological tissue distribution of ^{125}I-Labeled Compounds

Following the intravenous injection (i.v.) in the tail vein of 6 μCi (0.22 MBq) ^{125}I-labeled compounds (2.6 μmol), mice (n = 5) were killed after given time intervals. Aliquots of different tissue were weighed and immediately measured for radioactivity. Samples were counted in a gammatrac 1191 Tracor analytic counter. The tissue distribution was determined by calculating the relative concentration of ^{125}I activity in tissue. The time course of radioactivity was evaluated in terms of percentage of injected dose per g of tissue (%ID/g). Tumor/blood and tumoral/normal tissue ratios were also calculated.

Imaging

B16 melanoma-bearing C57BL6 mice or nude mice xenografted with human melanomas were injected with 60 μCi/mice *4*(c) (2.2 MBq) and used for imaging studies. Mice were anesthetized with pentobarbital 5% diluted to 1/5 in isotonic saline (0.1 ml intraperitoneal per mouse). They were scanned during 10 min with a gamma camera (gammatome II) fitted with a pinhole collimator of 3.36-mm aperture (sensitivity 1.1×10^{-4}) set at 80 mm from the animal. Images were taken from 1 to 24 hr postinjection and developed most of the time without additional background subtraction of computer enhancement. In addition to analog images, static views were acquired on a computer system (Sopha Medical, Buc, France) and stored on a disk for later analysis and display.

Statistical Analysis

The results of each point of our work were analyzed separately. Analysis comprised two or three factors of analysis of variance (ANOVA) (for independent series and with different subjects for each group), followed, where necessary, by Newman-Keuls post-hoc analysis. Significance levels were $p < 0.05$.

RESULTS

Autoradiography

Figure 3 presents autoradiograms obtained at 1 hr and 4 hr after intravenous injection of *4*(c) to mice bearing B16, M4Beu or M3Dau melanomas.

Tumoral Localization of the Four ^{125}I-Labeled Compounds

Compound Study. B16 melanoma uptake of each compound is shown in Figure 4. Values are expressed as percentage of injected dose per g of tumor. Data analysis gave a significant difference for Compound and Time and the post-hoc analysis showed these effects could be attrib-

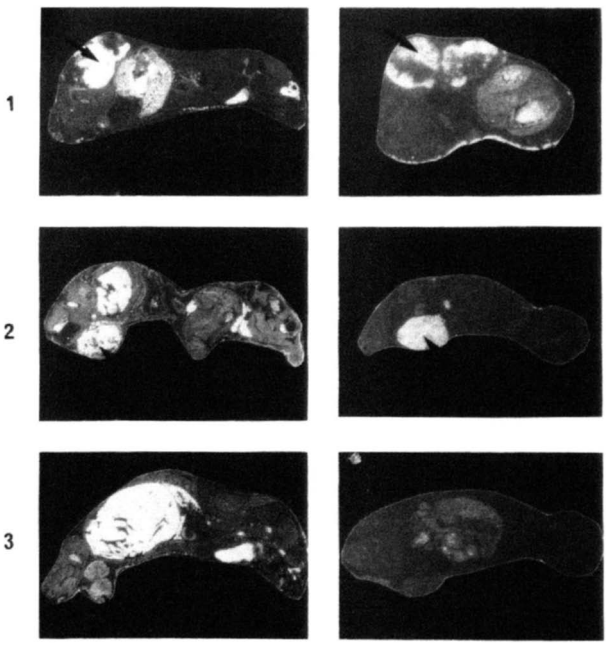

FIGURE 3. Autoradiograms of mice bearing B16 melanoma (1) or human melanoma heterotransplants (2, M4Beu and 3, M3Dau) at 1 hr (left) and 4 hr (right) after i.v. injection of *4*(c). Autoradiograms are presented as positive prints, which means that a white area corresponds with high activity in tne section.

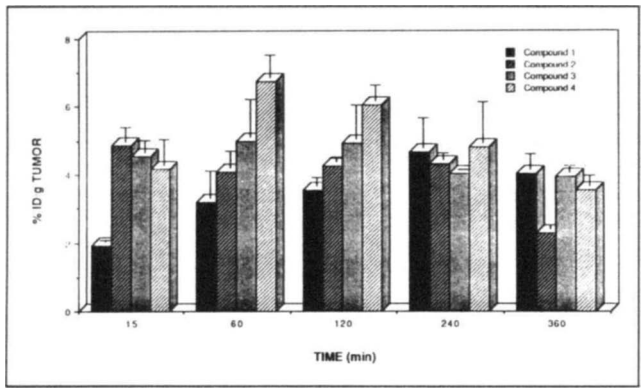

FIGURE 4. Tumoral concentration of four iodinated compounds in mice bearing B16 melanoma. The % ID/g tumor was determined from 15 to 360 min after i.v. injection.

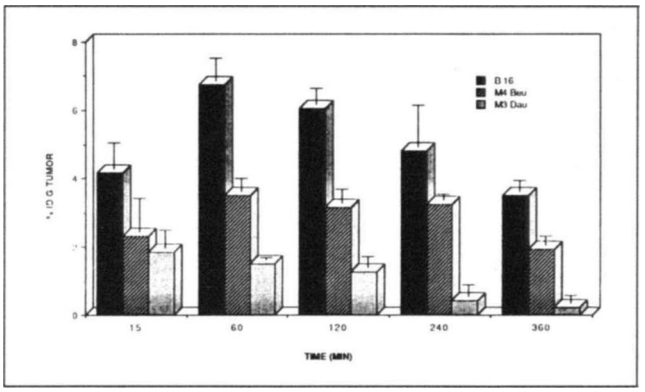

FIGURE 6. Tumor concentration of *4*(c) in mice bearing murine melanoma and in nude mice bearing human heterotransplant melanoma, either melanotic M4Beu or amelanotic M3Dau. The %ID/g tumor was determined from 15 to 360 min after i.v. injection.

uted to the following (/ means significant difference, and m is the average value of the corresponding factor):

$$4(c)\ (m = 5.08)/1(c)\ (m = 3.47).$$

Tumor-to-blood ratios of the four compounds are shown in Figure 5. The statistical analysis gave

$$4(c)\ (m = 8.63)/[1(c)(m = 1.36)\text{–}2(c)$$
$$\cdot(m = 1.31)\text{–}3(c)(m = 1.10)]$$

Tumor Study. Tumor uptake of compound *4*(c) for the two human melanoma heterotransplants compared to the uptake in the murine tumor is shown in Figure 6. Data were analyzed, and we obtained a significant difference for tumor and for time:

B16 (m = 5.07)/M4Beu(m = 2.84)/M3Dau(m = 1.07)

The tumor-to-blood ratios are shown in Figure 7. The studies showed

B16(m = 8.63)-M4Beu(m = 7.82)/M3Dau (m = 1.58).

Tissue Distribution of [^{125}I]-*N*-(2-Diethylaminoethyl) 4-Iodobenzamide

The results of biodistribution experiments evaluating *4*(c) in mice carrying three models of melanoma are presented in Tables 1–3. Metabolites may be involved, but only total radioactivity was measured in the various tissues so that the total of ^{125}I containing moities was estimated. For the three analyses of variance, one for each time (6, 12, and 24 hr), we observed (about percentages of injected dose per g of tissue): melanotic melanomas/(all the other tissues).

Comparative Study Between [^{125}I]IMP and [^{125}I]-*N*-(2-Diethylaminoethyl)-4-Iodobenzamide

Table 4 gives the tumor-to-tissue ratios for the three tumor models after injection of [^{125}I]IMP, same ratios after injection of *4*(c) appear in Tables 1–3. The main statistical results of all analyses of variance (one for each tumor)

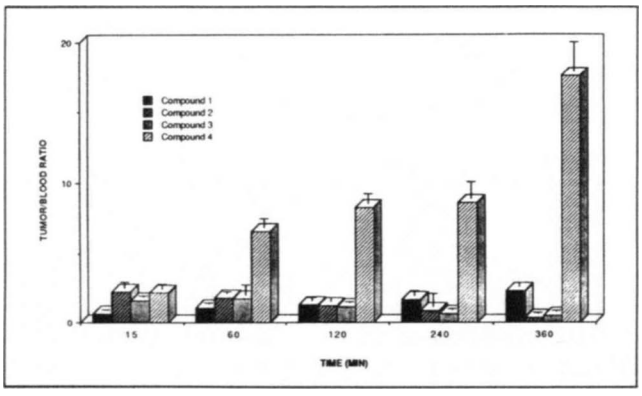

FIGURE 5. Tumor-to-blood ratios from 15 to 360 min after i.v. injection of the four iodinated compounds in mice bearing B16 melanoma.

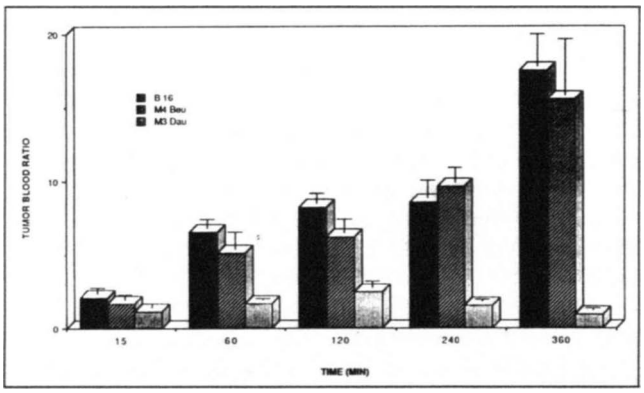

FIGURE 7. Tumor-to-blood ratios from 15 to 360 min after i.v. injection of *4*(c) in mice bearing murine melanoma and in athymic mice bearing human heterotransplant melanoma, either melanotic M4Beu or amelanotic M3Dau.

TABLE 1

Biodistribution and Some Tumor-to-Organ Ratios of [^{125}I]Iodobenzamide in C57BL6 Mice Bearing B16 Melanoma at Various Times After Injection (%ID/g; mean ± s.e.m., n = 5)

Tissue	1 hr	2 hr	4 hr	6 hr	12 hr	24 hr
Melanoma	6.75 ± 0.67	6.04 ± 0.47	4.82 ± 1.19	3.53 ± 0.31	1.01 ± 0.51	0.79 ± 0.09
Blood	1.04 ± 0.09	0.74 ± 0.04	0.54 ± 0.07	0.21 ± 0.02	0.06 ± 0.004	0.02 ± 0.01
Plasma	0.82 ± 0.07	0.55 ± 0.03	0.45 ± 0.03	0.21 ± 0.02	0.06 ± 0.006	0.02 ± 0.01
Liver	6.04 ± 0.40	4.02 ± 0.22	2.46 ± 0.52	0.95 ± 0.08	0.22 ± 0.01	0.16 ± 0.01
Kidney	8.56 ± 0.43	5.93 ± 0.58	3.67 ± 0.58	1.10 ± 0.09	0.15 ± 0.01	0.07 ± 0.01
Gut	5.22 ± 0.23	3.94 ± 0.32	2.80 ± 0.58	0.75 ± 0.13	0.10 ± 0.01	0.02 ± 0.01
Stomach	6.03 ± 0.75	3.87 ± 0.85	2.35 ± 0.59	1.14 ± 0.25	0.14 ± 0.02	0.07 ± 0.01
Lung	10.99 ± 0.97	6.12 ± 0.42	4.29 ± 0.85	1.99 ± 0.41	0.12 ± 0.008	0.05 ± 0.01
Brain	2.67 ± 0.31	1.40 ± 0.07	0.70 ± 0.08	0.32 ± 0.03	0.02 ± 0.002	0.005 ± 0.001
Thyroid*	0.066 ± 0.006	0.044 ± 0.004	0.036 ± 0.005	0.033 ± 0.004	0.01 ± 0.00	0.020 ± 0.001
Ratios						
Tumor/Blood	6.55 ± 0.60	8.23 ± 0.68	8.57 ± 1.21	17.58 ± 2.16	19.00 ± 10.54	37.33 ± 6.88
Tumor/Liver	1.12 ± 0.10	1.31 ± 0.25	1.98 ± 0.26	3.83 ± 0.48	4.65 ± 2.46	4.94 ± 0.65
Tumor/Lung	0.62 ± 0.05	0.99 ± 0.06	1.15 ± 0.16	2.13 ± 0.55	9.39 ± 5.30	15.82 ± 2.61
Tumor/Brain	2.57 ± 0.23	4.35 ± 0.35	6.85 ± 1.16	11.50 ± 1.45	46.11 ± 26.83	146.96 ± 13.17
Tumor/Muscle	4.72 ± 0.82	5.38 ± 0.41	7.32 ± 0.85	18.92 ± 2.38	48.04 ± 26.16	94.56 ± 13.36

* %ID/organ.

were a significant difference for compound and for time (6, 12, 24 hr):

	4(c)	IMP
B16	m = 32.97	m = 2.67;
M4Beu	m = 9.80	m = 2.63

For M3Dau, the analysis did not make clearer the significant differences that we observed for each factor.

Imaging Study of [^{125}I]-*N*-(2-Diethylaminoethyl)4-Iodobenzamide

Figure 8A shows a posterior view of C57BL6 mouse bearing a B16 melanoma on the right flank 6 hr postinjection of *4*(c). Figure 8B is the tumoral image of the same animal on the same position at the same time. Figures 9 and 10 present anterior view of athymic nude mice bearing human melanotic melanoma heterotransplants at 4 and

TABLE 2

Biodistribution and Some Tumor-to-Organ Ratios of [^{125}I]Iodobenzamide in Nude Mice Bearing Human Melanotic Melanoma (M4 Beu) Xenografts at Various Times After Injection (%ID/g; mean ± s.e.m., n = 5)

Tissue	1 hr	2 hr	4 hr	6 hr	12 hr	24 hr
Melanoma	3.51 ± 0.40	3.17 ± 0.40	3.25 ± 0.17	1.96 ± 0.24	0.36 ± 0.05	0.07 ± 0.01
Blood	0.87 ± 0.02	0.53 ± 0.06	0.32 ± 0.03	0.13 ± 0.02	0.02 ± 0.01	0.010 ± 0.002
Plasma	0.46 ± 0.02	0.35 ± 0.06	0.20 ± 0.02	0.12 ± 0.03	0.02 ± 0.01	0.010 ± 0.002
Liver	5.27 ± 0.22	3.50 ± 0.33	2.28 ± 0.16	0.94 ± 0.09	0.28 ± 0.03	0.13 ± 0.02
Kidney	7.63 ± 0.23	5.90 ± 0.69	4.28 ± 0.61	0.99 ± 0.14	0.10 ± 0.02	0.06 ± 0.02
Gut	3.76 ± 0.35	2.35 ± 0.30	1.56 ± 0.20	0.52 ± 0.12	0.08 ± 0.03	0.03 ± 0.01
Stomach	2.49 ± 0.07	1.51 ± 0.24	1.16 ± 0.12	0.49 ± 0.07	0.07 ± 0.02	0.04 ± 0.01
Lung	7.77 ± 0.17	4.71 ± 0.62	3.60 ± 0.27	1.25 ± 0.15	0.08 ± 0.02	0.05 ± 0.01
Brain	1.66 ± 0.10	1.13 ± 0.13	0.78 ± 0.05	0.28 ± 0.03	0.010 ± 0.002	0.006 ± 0.001
Thyroid*	0.058 ± 0.005	0.064 ± 0.009	0.050 ± 0.009	0.075 ± 0.009	0.066 ± 0.005	0.078 ± 0.002
Ratios						
Tumor/Blood	5.14 ± 1.15	6.25 ± 0.94	9.65 ± 1.06	15.58 ± 3.84	18.89 ± 1.90	6.24 ± 1.93
Tumor/Liver	0.86 ± 0.20	0.94 ± 0.15	1.38 ± 0.15	2.06 ± 0.07	1.24 ± 0.11	0.59 ± 0.13
Tumor/Lung	0.58 ± 0.14	0.73 ± 0.12	0.88 ± 0.11	1.89 ± 0.20	5.04 ± 0.71	1.84 ± 0.63
Tumor/Brain	2.67 ± 0.53	2.95 ± 0.45	4.12 ± 0.43	6.94 ± 0.25	21.20 ± 2.11	15.00 ± 5.22
Tumor/Muscle	3.49 ± 0.81	3.69 ± 0.67	6.19 ± 0.82	4.63 ± 0.54	25.31 ± 2.88	7.21 ± 2.57

* %ID organ.

TABLE 3
Biodistribution and Some Tumor-to-Organ Ratios of [^{125}I]Iodobenzamide in Nude Mice Bearing Human Amelanotic Melanoma Xenografts (M3 Dau) at Various Times After Injection (%ID/g; mean ± s.e.m., n = 5)

Tissue	1 hr	2 hr	4 hr	6 hr	12 hr	24 hr
Melanoma	1.51 ± 0.07	1.29 ± 0.30	0.45 ± 0.03	0.23 ± 0.02	0.07 ± 0.02	0.009 ± 0.001
Blood	0.89 ± 0.05	0.52 ± 0.04	0.29 ± 0.02	0.23 ± 0.02	0.06 ± 0.01	0.008 ± 0.001
Plasma	0.55 ± 0.04	0.33 ± 0.03	0.24 ± 0.02	0.24 ± 0.02	0.06 ± 0.01	0.007 ± 0.001
Liver	5.68 ± 0.62	3.35 ± 0.26	2.10 ± 0.28	1.10 ± 0.04	0.30 ± 0.01	0.10 ± 0.01
Kidney	8.39 ± 0.91	5.12 ± 0.46	2.15 ± 0.30	0.78 ± 0.03	0.14 ± 0.01	0.03 ± 0.01
Gut	3.74 ± 0.34	2.67 ± 0.33	1.10 ± 0.17	0.42 ± 0.04	0.27 ± 0.12	0.01 ± 0.01
Stomach	2.32 ± 0.17	1.85 ± 0.17	1.36 ± 0.35	1.17 ± 0.02	0.38 ± 0.09	0.03 ± 0.01
Lung	6.88 ± 0.84	5.63 ± 0.65	2.84 ± 0.39	0.76 ± 0.09	0.11 ± 0.01	0.02 ± 0.01
Brain	1.40 ± 0.11	0.99 ± 0.08	0.51 ± 0.06	0.20 ± 0.01	0.02 ± 0.01	0.002 ± 0.001
Thyroid*	0.060 ± 0.003	0.046 ± 0.002	0.044 ± 0.005	0.068 ± 0.010	0.044 ± 0.002	0.050 ± 0.010
Ratios						
Tumor/Blood	1.70 ± 0.03	2.47 ± 0.48	1.58 ± 0.14	0.97 ± 0.08	1.32 ± 0.49	1.17 ± 0.11
Tumor/Liver	0.28 ± 0.03	0.37 ± 0.06	0.23 ± 0.03	0.23 ± 0.02	0.26 ± 0.10	0.09 ± 0.01
Tumor/Lung	0.23 ± 0.02	0.24 ± 0.03	0.16 ± 0.01	0.30 ± 0.02	0.78 ± 0.34	0.38 ± 0.06
Tumor/Brain	1.09 ± 0.05	1.27 ± 0.20	0.91 ± 0.11	1.11 ± 0.11	2.86 ± 0.90	4.42 ± 0.59
Tumor/Muscle	1.19 ± 0.07	1.60 ± 0.28	1.44 ± 0.13	2.02 ± 0.19	3.41 ± 1.01	1.47 ± 0.16

* %ID/organ.

24 hr postinjection of *4*(c) (highest activity is corresponding to white).

DISCUSSION

Qualitative studies of autoradiography in B16 melanoma-bearing mice showed tumoral localization of radioactivity after injection of the four iodinated compounds. Compound *4*(c) produced the most intense tumoral images at each time interval postinjection (Fig. 3-1). High concentration was also observed in the other melanotic melanoma, M4Beu at 1 and 4 hr after injection of *4*(c) (Fig. 3-2). M3Dau only displayed a low activity 1 hr postinjection (Fig. 3-3). For the three tumor models, heterogeneous concentration of radioactivity corresponded to areas of necrosis of the tumor (with absence of uptake).

The first step of the tumoral B16 localization showed tumor uptake of the same order of magnitude for the four iodinated compounds. The highest tumor uptake (6.5% ID/g) was observed at 1 hr for compound *4*(c). The statistical analyses only allowed us to separate the compound *4*(c) from compound *1*(c) as extremes. For tumor-to-blood ratios, a significant difference appeared between *4*(c) and the three other compounds: *4*(c) quickly cleared from the blood and gave higher ratios from 1 to 6 hr postinjection. This explained the good autoradiographic images obtained

TABLE 4
Tumor-to-Organ Ratios After Intravenous Injection of [^{125}I]IMP in Mice Bearing Either B16 Melanoma or Melanotic and Amelanotic Human Melanoma Heterotransplants

Ratios	1 hr	2 hr	4 hr	6 hr	12 hr	24 hr	Melanoma
Tumor/Blood	7.35 ± 0.75	9.95 ± 1.23	7.19 ± 0.78	3.36 ± 1.62	5.27 ± 1.03	4.57 ± 0.94	
Tumor/Liver	0.70 ± 0.07	0.71 ± 0.05	0.74 ± 0.06	0.46 ± 0.22	1.22 ± 0.18	1.63 ± 0.43	
Tumor/Lung	0.49 ± 0.05	0.52 ± 0.02	0.47 ± 0.07	0.30 ± 0.18	0.48 ± 0.09	0.49 ± 0.14	B16
Tumor/Brain	0.56 ± 0.05	0.70 ± 0.05	0.80 ± 0.07	0.52 ± 0.29	1.40 ± 0.15	1.79 ± 0.53	
Tumor/Muscle	2.70 ± 0.35	3.31 ± 0.22	3.65 ± 0.27	2.13 ± 1.07	5.58 ± 0.65	6.35 ± 0.54	
Tumor/Blood	4.01 ± 0.46	6.97 ± 1.46	6.87 ± 0.85	5.81 ± 1.02	3.30 ± 0.32	3.59 ± 0.78	
Tumor/Liver	0.24 ± 0.03	0.45 ± 0.14	0.72 ± 0.06	0.74 ± 0.08	1.09 ± 0.12	1.29 ± 0.15	
Tumor/Lung	0.21 ± 0.01	0.39 ± 0.15	0.49 ± 0.07	0.42 ± 0.10	0.37 ± 0.04	0.39 ± 0.03	M4 Beu
Tumor/Brain	0.26 ± 0.02	0.50 ± 0.12	0.78 ± 0.08	0.79 ± 0.09	1.05 ± 0.10	1.29 ± 0.18	
Tumor/Muscle	1.62 ± 0.13	3.06 ± 0.68	4.56 ± 0.33	4.83 ± 0.65	5.94 ± 0.72	8.38 ± 1.12	
Tumor/Blood	4.03 ± 0.18	4.14 ± 0.29	3.27 ± 0.16	2.59 ± 0.22	1.44 ± 0.10	1.03 ± 0.09	
Tumor/Liver	0.21 ± 0.02	0.23 ± 0.02	0.30 ± 0.02	0.31 ± 0.01	0.33 ± 0.02	0.36 ± 0.02	
Tumor/Lung	0.18 ± 0.03	0.22 ± 0.02	0.19 ± 0.01	0.20 ± 0.03	0.16 ± 0.02	0.14 ± 0.01	M3 Dau
Tumor/Brain	0.26 ± 0.01	0.29 ± 0.01	0.32 ± 0.01	0.35 ± 0.01	0.35 ± 0.01	0.37 ± 0.02	
Tumor/Muscle	1.51 ± 0.14	1.77 ± 0.09	1.80 ± 0.07	2.26 ± 0.10	2.26 ± 0.10	2.19 ± 0.13	

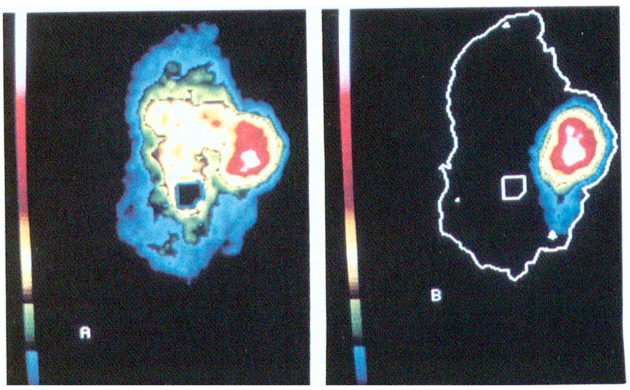

FIGURE 8. (A) Scintigram of a C57BL6 mouse bearing B16 melanoma in the right flank. Images were obtained with a pinhole collimator 6 hr postinjection. (B) Tumoral image at the same time showing preferential radioactive concentration of *4*(c) within the zones of the tumor itself.

after injection of compound *4*(c). The preliminary screening prompted us to perform more experiments with *4*(c).

We observed on Figure 7 that after injection of *4*(c) the tumoral uptakes are separated in two groups: the melanotic tumors, (B16 and M4Beu) and the amelanotic one (M3Dau). This has been confirmed by statistical analysis. This major uptake difference between pigmented and nonpigmented tumors suggests that the localization could be partly dependent on the synthesis of melanin.

In order to visualize malignant melanoma and metastases, a potential radiopharmaceutical must meet two criteria: high %ID/g tumor and high tumor/tissue ratios (blood, muscle, brain, liver or lung). One hour after intravenous injection of *4*(c), the ^{125}I activity was distributed over most tissues with preference for kidney, liver, lung and digestive tracts. We noted (Tables 1 and 2) a high amount of radioactivity in the melanotic tumors. Then a fast elimination was observed with a preferential retention of radioactivity in the melanomas. The statistical analysis showed a significant difference from 6 to 24 hr postinjection [% ID/g for B16 and M4Beu higher than %ID/g for all analyzed tissues]. The tumor versus blood ratios

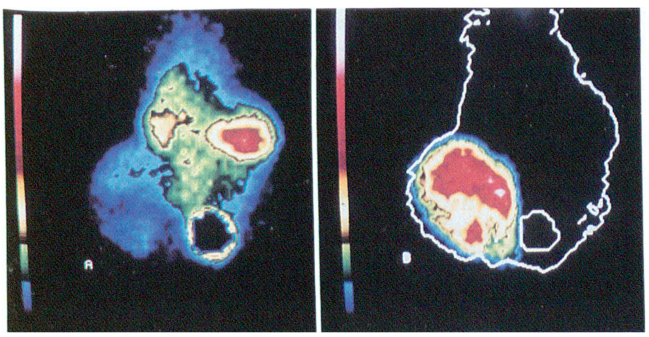

FIGURE 9. (A) Scintigram of a nude mouse xenografted with a human melanotic melanoma in the right flank. Images were obtained with a pinhole collimator 4 hr postinjection. (B) Tumoral image at 4 hr postinjection.

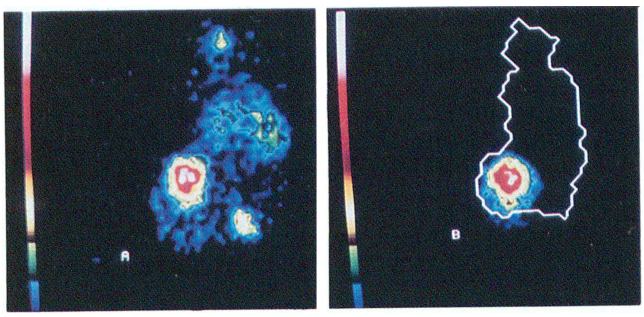

FIGURE 10. (A) Scintigram of a nude mouse xenografted with a human melanotic melanoma in the right flank. Images were obtained with a pinhole collimator 24 hr postinjection (B) Tumoral image at 24 hr postinjection.

reached a maximum for M3Beu at 12 hr postinjection and a maximum for B16 at 24 hr. A difference of kinetics appeared between the murine and human melanotic tumors. We also noted that ratios of tumor uptake to uptake in selected organs, which could be the location of metastases, were all greater than 1 from 6 to 24 hr.

Table 3 shows that M3Dau tumoral uptake was low at each time postinjection. We only noted particular values at 1 and 2 hr, which was probably related to blood activity. This confirmed the images obtained on autoradiography. The tumor/tissue ratios were always low due to the poor tumoral concentration.

It appeared from the tissue distribution that *4*(c) has potential as a melanoma imaging agent, firstly with high %ID/g melanotic melanomas, (with the same percentages significantly higher than those of all analyzed tissues) and secondly with high tumor/tissue ratios. The statistical analyses also allowed us to find the range of potential imaging times which seemed the best.

After intravenous injection of ^{125}I-IMP we observed a slow blood clearance. Until 24 hr post-injection the uptake in almost all analyzed tissues was higher than tumor. The statistical analysis of ratios in Table 4 comparatively to the same ratios after i.v. injection of *4*(c) (Tables 1 and 2) showed a significant difference between *4*(c) and IMP (for B16 and M4Beu). The differences were partly due to the quick blood clearance of *4*(c) versus the slow blood clearance of IMP. Therefore these comparative studies between IMP and *4*(c) at equivalent molar doses indicated than *4*(c) was a better radiotracer with in vivo models.

Until 24 hr after injection of IMP, the high radioactivity in all tissues made it impossible to obtain melanoma images with good contrast. Because of the accumulation of *4*(c) within the melanotic melanomas, it was possible to image the tumors with a noninvasive procedure. We noted a substantial accumulation of radioactivity in the digestive tract, in the bladder and in the tumor during the first hours postinjection (Fig. 9), but from 6 to 24 hr a quick blood clearance and the adequate tumor uptake resulted in a clear delineation of the tumor masses from other tissues (Fig. 8). The 24-hr scintigram (Fig. 10) pro-

vides a clear view of the tumor with virtually no blood or intestinal radioactivity. As we noted on autoradiographs, we had no uptake into areas of necrosis. This preferential localization within the zones of the tumor itself is of particular interest for clinical imaging.

CONCLUSION

N-(2-diethylaminoethyl)4-iodobenzamide is a new type of radioiodinated compound which is significantly taken up by melanotic melanomas. The mechanism of tumor uptake is presently under investigation. It remains to be seen whether ^{123}I-labeled compound would show similar results. It is obvious that only studies in man would elucidate these points. Preclinical toxicology studies and analytical expertises have been performed. The study has received the approval of our Institutional Ethical Committee. The preliminary clinical evaluation of the ^{123}I radiopharmaceutical provides evidence that it represents a useful imaging agent for detection of primary malignant melanoma and metastases.

ACKNOWLEDGMENTS

The authors gratefully thank Mrs. J. Lefrançois for secretarial assistance. Special thanks are given to R.J. Ferguson for helpful comments on the manuscript. This research was supported in part by grants from the Federation Nationale des Centres de Lutte contre le Cancer and the Association pour la Recherche sur le Cancer.

REFERENCES

1. Lejeune FJ. Epidemiology and etiology of malignant melanoma. *Biomed Pharmacother* 1986;40:91–99.
2. Monk BE, Neill SM, du Vivier A. Missed malignant melanomas. *Br Med J* 1986;292:1000–1001.
3. Beaumier PL, Krohn KA, Carrasquillo JA, et al. Melanoma localization in nude mice with monoclonal Fab against p 97. *J Nucl Med* 1985;26:1172–1179.
4. Rosenblum MG, Murray JL, Hayne TP, et al. Pharmacokinetics of ^{111}In-labeled anti-p97 monoclonal antibody in patients with metastatic malignant melanoma. *Cancer Res* 1985;45:2382–2386.
5. Halpern SE, Dillman RO, Witztum KF, et al. Radioimmunodetection of melanoma utilizing In-111 96.5 monoclonal antibody: A preliminary report. *Radiology* 1985;155:493–499.
6. Buraggi GL, Callegar OL, Mariani G, et al. Imaging with ^{131}I-labeled monoclonal antibodies to a high molecular weight melanoma associated antigen in patients with melanoma efficacity of whole immunoglobulin and its F (ab')$_2$ fragments. *Cancer Res* 1985;45:3378–3787.
7. Larson SM. Lymphoma, melanoma, colon cancer: Diagnosis and treatment with radiolabeled monoclonal antibodies. *Radiology* 1987;165:297–304.
8. Taylor A, Milton W, Emre H, et al. Radioimmunodetection of human melanoma with Indium 111-labeled monoclonal antibody. *J Nucl Med* 1988;29:329–337.
9. Eary JF, Schroff RW, Abrams PG, et al. Successful imaging of malignant melanoma with Technetium-99m labeled monoclonal antibodies. *J Nucl Med* 1989;30:25–32.
10. Milder MS, Frankel RS, Bulkey GB, et al. Gallium-67 scintigraphy in malignant melanoma. *Cancer* 1973;32:1350–1356.
11. Hoffer P. Status of Gallium-67 in tumor detection. *J Nucl Med* 1980;21:394–398.
12. Kloster G, Bockslaff H. L-3-^{123}I-methyltyrosine for melanoma detection: a comparative evaluation. *Int J Nucl Med Biol* 1982;9:259–269.
13. Turner JH, Maziere M, Comar D. Localization of ^{11}C-radiopharmaceuticals in the Greene melanoma of hamsters. *Eur J Nucl Med* 1985;10:392–397.
14. Visser GW, Zwaagstra O, Gorree GC, et al. Synthesis and tumour localizing properties of [^{18}F]-5-fluoro-cytosine-arabinoside and [^{18}F]-5-fluorocyclocytidine. *Eur J Nucl Med* 1986;12:137–140.
15. Langevelde A van, Bakker CNM, Boer H, et al. Potential radiopharmaceuticals for the detection of ocular melanoma. Part II. Iodoquinoline derivatives and ^{67}Ga citrate. *Eur J Nucl Med* 1986;12:96–104.
16. Lambrecht RM, Packer S, Wolf AP, et al. Detection of ocular melanoma with 4-(3-dimethylaminopropyl-amino)-7-[^{123}I]-iodoquinoline. *J Nucl Med* 1984;25:800–804.
17. Coderre JA, Packer S, Fairchild RG, et al. Iodothiouracil as a melanoma localizing agent. *J Nucl Med* 1986;27:1157–1164.
18. Langevelde A van, Bergman W, Feitsma RJ, et al. A patient study with radioiodine labeled 5-iodo-2-thiouracil. *Eur J Nucl Med* 1988;14:640–641.
19. Wada M, Ichiya Y, Katsuragi M, et al. Scintigraphic visualization of human malignant with N-isopropyl-P-[I-123] iodoamphetamine. *Clin Nucl Med* 1985;10:415–417.
20. Cohen MB, Saxton RE, Lake RR, et al. Detection of malignant melanoma with iodine-123 iodoamphetamine. *J Nucl Med* 1988;29:1200–1206.
21. Moreau MF, Parry D, Michelot J et al. Synthèse, étude chez le rat, de composés radioiodés utilisables pour l'exploration du système nerveux central. *Eur J Med Chem* 1986;21:423–431.
22. Yeh SD, Helson L, Grando R. Tumor-localizing radionuclides in heterotransplanted human tumors in nude mice. *Int J Nucl Med Biol* 1979;6:169–173.
23. Chatal JF, Diez E, Guihard D. Is the nude mouse bearing a human tumor the best model for study of tumor-localizing radionuclides? *Int J Nucl Med Biol* 1981;8:181–183.
24. French patent no. P.V. 8901898, 02/14/1989.
25. Seevers RH, Counsell RE. Radioiodination techniques for small organic molecules. *Chem Rev* 1982;82:575–590.
26. Benedict DR, Bianchi TA, Cate LA. Synthesis of simple unsymmetrical ethers from alcohols and alkyl halides or sulfates: The potassium hydroxide/dimethyl sulfoxide. *Syst Synth* 1979;6:428–429.
27. Jacubovich R, Dore JF. Tumour-associated antigens in culture medium of malignant melanoma cell strains. *Cancer Immunol Immunother* 1979;7:59–64.
28. Jacubovich R, Cabrillat H, Gerlier D, et al. Tumourigenic phenotypes of human melanoma cell lines in nude mice determined by an active antitumour mechanism. *Br J Cancer* 1985;51:335–345.
29. Ullberg S. The technique of whole-body autoradiography: Cryosectioning of large specimens. In: Alvfeldt O, ed. *Science tools*. Sweden: LKB Produkter AB; 1977:2–29.